Atmos. Chem. Phys., 11, 1659–1670, 2011
www.atmos-chem-phys.net/11/1659/2011/
doi:10.5194/acp-11-1659-2011

Atmospheric Chemistry and Physics

Assessing the regional surface influence through Backward Lagrangian Dispersion Models for aircraft CO_2 vertical profiles observations in NE Spain

A. Font[1,2,*], **J.-A. Morguí**[1,2], **and X. Rodó**[1,3]

[1]Institut Català de Ciències del Clima, Dr. Trueta 203, 08005, Barcelona, Catalonia, Spain
[2]Laboratori de Recerca del Clima, Parc Científic de Barcelona, Universitat de Barcelona, Baldiri i Reixach, 2, 2a planta, 08028, Barcelona, Catalonia, Spain
[3]Institució Catalana de Recerca i Estudis Avançats, Passeig Lluís Companys, 23, 08010, Barcelona, Catalonia, Spain
[*]now at: Environmental Research Group, King's College London, 150 Stamford Street, London, SE1 9NH, UK

Received: 4 January 2010 – Published in Atmos. Chem. Phys. Discuss.: 29 March 2010
Revised: 28 January 2011 – Accepted: 7 February 2011 – Published: 21 February 2011

Abstract. In this study the differences in the measured atmospheric CO_2 mixing ratio at three aircraft profiling sites in NE Spain separated by 60 km are analyzed in regard to the variability of the surface fluxes in the regional surface influence area. First, the Regional Potential Surface Influence (RPSI) for fifty-one days in 2006 is calculated to assess the vertical, horizontal and temporal extent of the surface influence for the three sites at the regional scale (10^4 km^2) at different altitudes of the profile (600, 1200, 2500 and 4000 meters above the sea level, m a.s.l.). Second, three flights carried out in 2006 (7 February, 24 August and 29 November) following the Crown Atmospheric Sampling (CAS) design are presented to study the relation between the measured CO_2 variability and the Potential Surface Influence (PSI) and RPSI concepts. At 600 and 1200 m a.s.l. the regional signal is confined up to 50 h before the measurements whereas at higher altitudes (2500 and 4000 m a.s.l.) the regional surface influence is only recovered during spring and summer months. The RPSI from sites separated by ∼60 km overlap by up to 70% of the regional surface influence at 600 and 1200 m a.s.l., while the overlap decreases to 10–40% at higher altitudes (2500 and 4000 m a.s.l.). The scale of the RPSI area is suitable to understand the differences in the measured CO_2 concentration in the three vertices of the CAS, as CO_2 differences are attributed to local surrounding fluxes (February) or to the variability of regional surface influence as for the August and November flights. For these two flights, the variability in the regional scale influences the variability measured in the local scale. The CAS sampling design for aircraft measurements appears to be a suitable method to cope with the variability of a typical grid for inversion models as measurements are intensified within the PBL and the background concentration is measured every $\sim 10^2$ km.

Correspondence to: A. Font
(afont@ic3.cat)

1 Introduction

Atmospheric measurements show that the CO_2 concentration in the atmosphere is currently ∼387 ppmv; but this global average must be downscaled to understand the regional distribution of CO_2 emissions (Marquis and Tans, 2008). Improving our understanding of the carbon cycle at various spatial and temporal scales will require the integration of multiple, complementary and independent methods used by different research communities (Canadell et al., 2000; Gerbig et al., 2009). The assessment of CO_2 surface fluxes has been traditionally studied at two spatial scales: the local and the global (Lafont et al., 2002). Bottom-up approaches process local fluxes inferred for example by eddy covariance systems placed mainly on forests and/or grass lands (e.g. Baldocchi et al., 2001) which provide estimates of carbon fluxes at fine spatial scales (10^1–10^2 km), and scale them up to the global or regional scale using oriented or diagnostic models (e.g. Papale and Valentini, 2003) or by satellite information (Running et al., 2004). Top-down approaches are based instead on atmospheric inverse transport studies and use CO_2 measurements on remote sites, inverse numerical methods and satellite data (e.g. Ciais et al., 1995; Fan et al., 1998; Bousquet

et al., 1999; Gurney et al., 2002, 2008; Peters et al., 2009). However, global inversions do not provide much spatial resolution nor do they have the potential to increase the current understanding of the terrestrial processes at the regional scale responsible for the future control of fluxes (Canadell et al., 2000). The CO_2 concentration over continents shows large variability resulting from surface fluxes which vary both spatially across the landscape in close relation to vegetation types and conditions (Gerbig et al., 2003a; Sarrat et al., 2007a; Choi et al., 2008); and temporally due to signal reversal of biospheric fluxes between night (respiration) and day (photosynthesis) combined with strong daily mixing within the planetary boundary layer (Gloor et al., 2001; Lafont et al., 2002; Gerbig et al., 2008; Denning et al., 2008). In addition, CO_2 variability over continents is also linked to synoptic and mesoscale changes in meteorological conditions (Sidorov et al., 2002; Shashkov et al., 2007; Ahmadov et al., 2009). The interpretation of these mixing ratios is therefore linked to the knowledge of surface fluxes around the measurement site and at a regional scale (Lin et al., 2004).

Regional fluxes are estimated by analyzing vertical profiles of concentration collected at one location from tall towers (i.e. Bakwin et al., 2003), from aircraft vertical sampling (Wofsy et al., 1988; Lloyd et al., 2001; Font et al., 2010) or by performing Lagrangian boundary layer budget campaigns (Schmitgen et al., 2004; Martins et al., 2009; Sarrat et al., 2009). The estimation of the regional surface fluxes based on a single tall tower is restrained by the influence of local fluxes (of up to 50 km distance) (Gerbig et al., 2009). Aircraft profiling characterizes the vertical distribution of the CO_2 concentration from the near surface up to the free troposphere. The further from the ground measurements are taken, the less they are influenced by local processes. Therefore, measurements obtained at higher altitude are more representative of a mean regional surface flux.

Mesoscale models have been developed in recent years to assess regional CO_2 variability that encompass the distribution of sources and sinks of carbon at this relevant scale. Inverse methods to infer regional surface fluxes are limited by the resolution of atmospheric transport models and by the availability of mixing ratios (Lin and Gerbig, 2005). However, the number of mesoscale campaigns to measure the CO_2 concentration and its variability at the regional scale has increased in the latest years (Dolman et al., 2006, 2009; Sarrat et al., 2009; Sun et al., 2010). These campaigns are used to validate mesoscale models but uncertainties are still large (Sarrat et al., 2007b) mainly due to mesoscale flows (i.e. topography, sea-land breezes) and representation errors. Representation error is introduced by the assumption that a point observation can be represented by the mean CO_2 mixing ratio of a model grid box (Tolk et al., 2008) and is associated with the strong CO_2 horizontal gradient over the continents due to the variation of land use and topography. Previous studies have quantified the scales of variability of atmospheric CO_2 and the related representation error in coarse resolution models, starting with statistical analysis of spatially distributed CO_2 aircraft data (Gerbig et al., 2003b; Lin et al., 2004), sensitivity analysis using different scales of variability of surface fluxes (Gerbig et al., 2003b) and statistical analysis of high resolution simulations of atmospheric CO_2 (van der Molen and Dolman, 2007; Corbin et al., 2008; Tolk et al., 2008).

The Crown Atmospheric Sampling (CAS, previously described in Font et al., 2008) was designed to provide a good characterization of the mean CO_2 concentration and its variability within the boundary layer in the central part of the Ebre watershed related to regional surface fluxes, as well as the characterization of the free troposphere concentration as a background value in a grid of 60 km × 60 km. In addition to vertical profiles in the vertices of a prism, horizontal transects at 600 and 1200 m a.s.l. complement the study of the spatial variability in the area. The aim of this paper is to study the vertical, horizontal and temporal extent of the regional surface influence area (10^4 km^2) that would have an impact on the CO_2 measurements carried out in vertical profiles using the CAS, examined through the concept of the footprint area. The footprint concept around a measurement site has been widely used to quantify from where and to what extent fluxes within the surrounding areas influence trace gas observations (Gloor et al., 2001). It is therefore a representation of the sensitivity of mixing ratios at measurement locations to upstream fluxes at prior times (Gerbig et al., 2009). It varies with height, but also with the wind direction, meteorological conditions (stability) and the magnitude of the CO_2 fluxes (Rannik et al., 2000; Aubinet et al., 2001).

The present study is organized as follows: the vertical, horizontal and temporal extent of the footprint area or the Potential Surface Influence (PSI) and the Regional Potential Surface Influence (RPSI) for a set of fifty-one days in 2006 for the three aircraft sites at four altitudes (600, 1200, 2500 and 4000 m a.s.l.) are examined in Sect. 3.1, 3.2 and 3.3 respectively. The extent of the regional surface influence area and its variability between sites for the flights done on 7 February, 24 August and 29 November 2006 is discussed in Sect. 4. Abbreviations used on this manuscript are: DJF for December, January and February; MAM for March, April and May; JJA for June, July and August; and SON for September, October and November.

2 Methods

2.1 Aircraft surveys

The aircraft sites measuring atmospheric CO_2 concentrations belong to the Spanish network ICARO and are sampled following the Crown Aircraft Sampling (CAS) previously described in Font et al. (2008). CAS samples CO_2 mixing ratios continuously in the vertices of an approximate 60 km × 60 km × 60 km prism, integrating vertical profiles from 600 to 2500 and 4000 m a.s.l. with horizontal transects

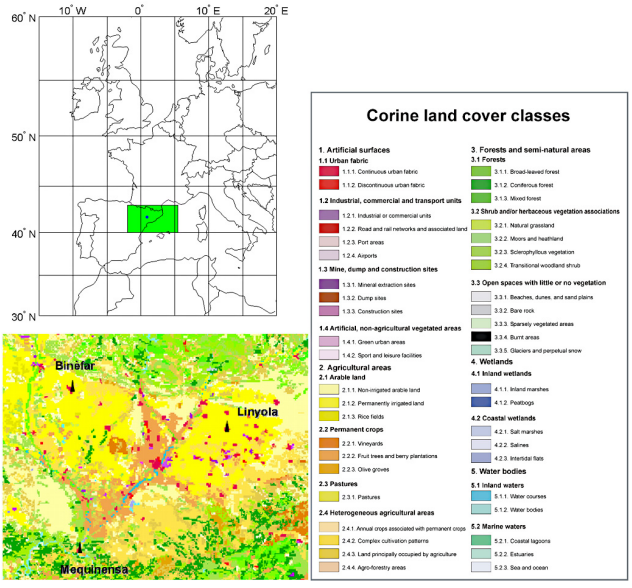

Fig. 1. Location map of the Linyola's area and the land uses around each vertex belonging to the CAS (Linyola, Mequinensa and Binefar) according to CORINE2000 database (European Environment Agency; http://www.eea.europa.eu/data-and-maps/data/corine-land-cover-2000-clc2000-seamless-vector-database)

at 600 and 1200 m a.s.l. The CO_2 concentration measured is related to the intensity of the underlying fluxes and the weather conditions. The first site where the CAS was implemented was around the Linyola's area in February 2006 (vertices of the CAS are Linyola – 41.8° N 0.9° E-, Mequinensa – 41.3° N 0.3° E- and Binefar –41.8° N 0.3° E; see Fig. 1). The CAS location was chosen as being representative of intensively irrigated land in the Ebre watershed.

2.2 Potential Surface Influence (PSI) and Regional Potential Surface Influence (RPSI)

The Lagrangian Particle Dispersion Models (LPDMs) are well-suited to delineate contributions from upwind source regions (Blanchard, 1999) at different spatial scales. The calculation of the PSI in this study is derived from the FLEXPART model. It simulates long-range and mesoscale transport, diffusion, dry and wet deposition, and radioactive decay of tracers released from point, line, area or volume sources (Stohl et al., 2005). The model parameterizes turbulence in the boundary layer and in the free troposphere by solving Langevin equations (Stohl and Thompson, 1999). LPDM backward simulations replace the traditional backward trajectory calculations as they account not only advection but also turbulence, convection and large-scale advection (Stohl et al., 2002; Seibert and Frank, 2004). FLEXPART is driven by global model-level data from the National Oceanic and Atmospheric Administration – National Centers for Environmental Prediction – Global Forecast System (NOAA-NCEP-GFS) with a horizontal resolution of $1° \times 1°$ and 26 vertical layers and a time resolution of 3 h (analyses at 00:00, 06:00, 12:00, 18:00 UT; forecasts at 03:00, 09:00, 15:00 and 21:00 UT). Ten thousand particles are released at 12:00 UT and transported four days back in time by the resolved winds and by parameterized subgrid and convection motions. The majority of studies aiming the characterization of the source areas of CO_2 measurements are based on backtrajectories analysis of 2 days (Taubman et al., 2006), 5 days (Aalto et al., 2002; Apadaula et al., 2003) or 7 days (Lloyd et al., 2002, 2007). Jorba et al. (2004) chose backtrajectories of 4 days to describe the tropospheric circulation at Barcelona as they were representative enough of the long-range transport and their error remained controlled. Here, as the objective is the assessment of the regional influence on CO_2 measurements rather than the long-range transport, we have also chosen 4 days as representative of this scale. The release points are defined as small boxes round the measurement sites with dimensions $0.01° \times 0.01° \times 10$ m. The size of the release box is chosen in accordance with the dimensions of the spiral drawn by the aircraft around the site (vertex of the CAS) when doing the vertical profiles. The model output ($120 \times 110 \times 16$ grids with a horizontal resolution of $0.5° \times 0.5°$; 16 vertical levels from ground up to 3000 m above ground level (m a.g.l.); temporal resolution of 3 h) consists of a response function related to the particles residence time (R_t) in each grid. The horizontal resolution of the grid cells in the output files ($0.5° \times 0.5°$) is chosen based on the distance between two aircraft measurement sites. It is assumed that the R_t in one grid cell is proportional to the source contribution to the mixing ratio at the measurement site.

The LPDM FLEXPART is used to assess the upwind source region of the three CO_2 vertical profiling sites (Linyola (LIN), Mequinensa (MEQ) and Binèfar (BIN); see Fig. 1) at four different altitudes (release altitudes at 600, 1200, 2500 and 4000 m a.s.l.) for 51 days in 2006. For each individual simulation the Potential Surface Influence (PSI) region is calculated to assess the upwind surface source region. The PSI is defined as the layer adjacent to the surface (0–300 m a.g.l.) where air masses reside before arriving at the measurement site, expressed in seconds. The thickness of the PSI is chosen as it is within the Planetary Boundary Layer (PBL) most of the time and it is high enough to allow large number of particles to be sampled (Stohl et al., 2003). Although the PBL height could be lower than 300 m a.g.l. in the region, especially in winter nights, the thickness of the PSI is a commitment threshold between the aforementioned factors. In this study, the PSI is a property function of the transport of air masses and it is independent of the intensity of surface fluxes.

A residence time threshold criteria is applied with the aim to assess the regional scale (10^4 km^2) of upwind surface source regions (RPSI) for the aircraft sites. Surface fluxes in the RPSI area are expected to create a detectable change

in the measured CO_2 concentration at the receptor site. The RPSI concept is similar to the "catchment area" exposed in Henne et al. (2010). Taking the maximum and the minimum surface fluxes values (diurnal and 3-hourly values) from the European assimilation system CarbonTracker for 2006 (Peters et al., 2007, 2009), the time required to detect a change in the measured concentration of 1ppmv (4σ the noise of the instrument used in this study) is ∼500 s. The grid cells with R_t greater than 500 s are expected to be those which potentially contribute the most to the variability at the measurements sites.

The ratio between mixing ratio and residence time in the PSI used in this study (1 ppmv/500 s = 2×10^{-3} ppmv s^{-1}) is situated in the range of values reported by Paris et al. (2010) that were obtained from direct regressions of CO_2 aircraft measurements over Siberia against residence time in the surface layer. That study reported values between 5×10^{-5} ppmv s^{-1} and 5×10^{-2} ppmv s^{-1} depending on the origin of air masses (local versus air masses advected from China) and the season in which the flight took place. The approach used here lies within the large range of values reported in Paris et al. (2010) found when air masses carried out the signal from areas with large surface fluxes (i.e. China). As the RPSI area for the measurements reported in this study is Europe, large ppmv s^{-1}ratios are also expected.

Considering this residence time threshold value and selecting those surface grid cells having a mean residence time greater than 500 s, the PSI area shrinks by 99.2% of its original value. The order of magnitude of the PSI area is the European continent ($\sim 1 \times 10^7$ km^2) and the RPSI is the Ebre watershed (8.6×10^4 km^2). Therefore, the application of this residence time threshold criteria is a valid method to assess the regional surface influence of atmospheric observations. From this point, the term PSI represents the Potential Surface Influence without applying any residence time threshold and RPSI represents the surface influence area defined by the grid cells with a residence time greater or equal to 500 s.

3 Footprints

3.1 Vertical range of the surface upwind sources for aircraft measurement sites

The residence time at different altitudes of the lower troposphere for air masses travelling to the receptor sites is studied by dividing the vertical model output in five levels: from 0 to 300 m (L1), from 301 to 800 (L2), from 801 to 1200 (L3), from 1201 to 3000 (L4), and above 3000 m a.g.l. (L5; out of the model output domain). The first layer (L1) is the same as defined by the PSI and is considered to be within the planetary boundary layer (PBL), and hence closely influenced by terrestrial or marine surface carbon fluxes. Conversely, the last two layers (L4 and L5) are considered to belong mostly to the free troposphere (FT). L2 and L3 are situated in a middle zone situated either in the PBL, the Entrainment Zone (EZ) or the FT, depending on the time of the day and on the weather conditions. Figure 2a summarizes the mean percentage of the residence time of air masses in each of the five layers considered at every 3 h time step for the three aircraft sites. Air masses reside more time in L1 (PSI) as lower release points are situated at the very beginning of simulations.

For releases at 600 m a.s.l., the residence time in L1 (PSI) is ∼30% of the simulation time (3 h) at the very first time step of the model output (3 h back), decreasing to 10% at 96 h back. For releases at high altitudes, the residence time in the PSI is very short: ∼5% at 2500 m a.s.l. and less than 1.5% at 4000 m a.s.l. all along the 96 h simulation. For releases started at 4000 m a.s.l., air masses are encountered outside the output domain (L5) most of the simulation time (∼85%). Seasonally, the percentage of R_t in the PSI for simulations starting at 600 m a.s.l. is higher during DJF and SON. For the first three hours of simulation, air masses remain more than 40% of the simulation time (DJF) and 35% (SON) in L1 and this value decreases to ∼20% for MAM and JJA. For simulations starting at 2500 and at 4000 m a.s.l., the percentage of R_t in L1 is higher during MAM and JJA (reaching percentages of 10% and 5%, respectively) rather than DJF and SON (less than 5% and 2%, respectively).

The distribution of the percentage of R_t in the PSI (L1) is related to the seasonality of atmospheric stability. During warm months, the convective boundary layer enhances intensive downward and upward motions leading to a well-mixed PBL. Convection acts as a scattering factor for particles, distributing them randomly in the PBL whereas during DJF and SON, inversions occur more often, suppressing the vertical transport near the surface and within the PBL. The vertical transfer of air masses in summer is faster than in winter more than a factor of 5 (Liu et al., 1984). During DJF and SON, the higher frequency of fronts and the uplift motions associated with them enhances the transfer of particles from lower layers up to higher ones. The transfer of particles from L5 or L4 to lower layers during warm months is associated to subsidence processes associated to anticyclonic weather. Therefore, gradients observed above the PBL might be attributed to surface fluxes over continental areas in MAM and JJA.

On average, the ground influence is almost lost at 2500 m a.s.l., confining the local, regional and elsewhere surface influence to below that altitude. CO_2 measurements at higher altitudes belong to a well-mixed latitudinal concentration not influenced by the short-term local and regional surface processes. Therefore, measurements taken at this altitude (or higher) are frequently used as boundary conditions (Gerbig et al., 2003b) even if continental-scale surface fluxes signals could be detected at high altitudes.

Those PSI grid cells having R_t <500 s are attributed to the outside regional domain (horizontal scale larger than 10^4 km^2). If CO_2 fluxes (both regional and elsewhere) were spatially homogenous, the regional part of the PSI (that is, the RPSI) would explain ∼40% of the variability of CO_2

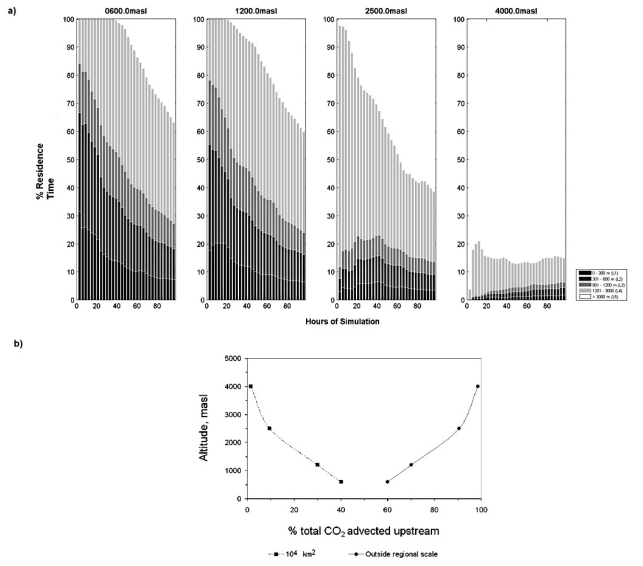

Fig. 2. (a) Temporal distribution of the percentage of Residence Time (R_t) at each 3 h time step at different layers of the low troposphere (0–300 or L1, 301–800 or L2, 801–1200 or L3, 1201–3000 or L4 and above 3000 m a.g.l., L5) for simulations started at 600, 1200, 2500 and 4000 m a.s.l. **(b)** Vertical distribution of the percentage of the regional surface influence (10^4 km^2) and outside the regional domain for the CO_2 vertical profiles belonging to the Linyola's CAS.

observed at the receptor; ∼30% at 1200 m a.s.l.; ∼9.5% at 2500 m a.s.l. and ∼1.5% at 4000 m a.s.l. (Fig. 2b). As expected, going up in the vertical profile, the CO_2 contribution from external sources is larger than at low levels. Measurements carried out below 2500 m a.s.l. are required for a good characterization of the surface fluxes and their spatial and temporal variability in the immediate proximity of observatories measuring atmospheric concentrations.

The fact that the RPSI influence accounts for 40% of the total variability of the entire PSI has an impact when modeling CO_2 mixing ratios: a bias in the fluxes from the RPSI area would have almost the same effect as the bias caused by the fluxes from the outside the domain.

3.2 Horizontal extent of the regional upwind sources for aircraft measurement sites

A classification of the grid cells to configure the regional surface influence area of a single atmospheric site is assessed by Principal Component Analysis (PCA). PCA, similar to eigenvector analysis or empirical orthogonal function analysis, has been used in studies to determine the spatial pattern of meteorological variables (Overland and Preisendorfer, 1982) and air pollution (Ashbaugh et al., 1984). PCA is a quantitative method that aims to reduce the number of variables describing a data set with several observations. The method generates a new set of variables or principal components (PC). Each PC is a linear combination of the original variables and all PCs are orthogonal to each other, so there is no redundant information. Here, the original variables are the set of 51 LPDM backward simulations for 2006 calculated using FLEPXART (j, from 1 to 51); the observations are the residence time (R_t) in each of the grid cells defining the RPSI (i-grid cells). The original matrix is composed by $(R_t)_{i,j}$. The application of the PCA to the original data thereby classifies the grid cells that compose the RPSI for each of the three aircraft sites keeping the maximum of variability without redundant information. The first (PC1) and second principal component (PC2) combined explain 75% of the original variance of the entire data set. Furthermore, the scree plot (not shown) indicates a sharp decrease of the variance explained by the following PCs. The variability explained by PC1 varies for each site, from 44% for MEQ; to 74% for BIN. The variability explained by PC2 is approximately 15% for LIN and MEQ; and approximately 6% for BIN.

The classification of the RPSI grid cells as a function of the new variables (or PCs) is shown in Fig. 3. The unit of the color scale is minutes; negative values for PC2 indicate that a number of RPSI grid cells are incompatible with others. PC1 separates the very local grid cells from the regional ones. PC2 classifies the RPSI grid cells depending on the synoptic situations linked to the main wind directions for each site. PC2 separates those grid cells from the E weather patterns against those one from W directions for BIN and LIN; and those from NE against SW for MEQ.

Similar patterns are retrieved when checking the altitude influence when PCA was carried out for the RPSI for simulations centered at 1200 m a.s.l. However, no spatial patterns are seen when carrying out the same analysis for the RPSI at 2500 and 4000 m a.s.l. as the surface influence is scattered (as discussed in Sect. 3.1).

Figure 3 represents the mean sensitivity surface area for each site. The different modes of variability classify the RPSI grid cells into local ones (PC1) or grid cells associated with a weather pattern (PC2). It presents the advantage of classifying the RPSI grid cells (local against regional; and different regional RPSI grid cells associated with some weather patterns). The PCA method highlights that there are combinations of RPSI grid cells which are disjointed in space, that is, there are impossible RPSI grid cell configurations. The classification of the RPSI grid cells enhances the contribution of CO_2 differences between sites to local or regional surface fluxes (see Sect. 4).

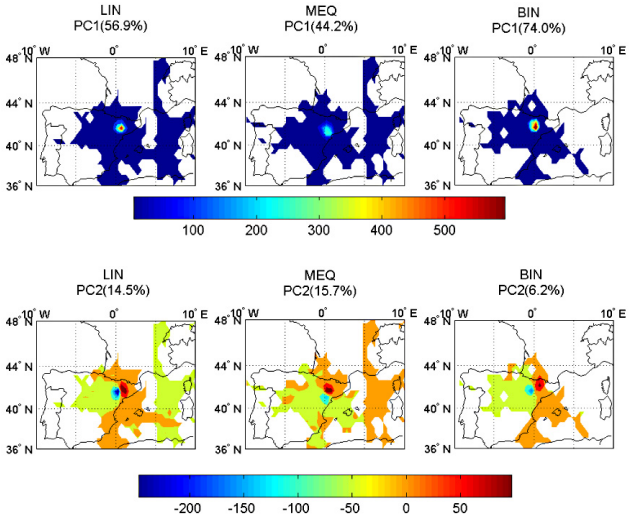

Fig. 3. Maps resulting from Principal Component Analysis (PCA) applied to an original matrix composed by the residence time in the RPSI grid cells (observations) for 51 backward simulations for 2006 (variables) for each of the three sites belonging to the Linyola's CAS. The classification of the RPSI grid cells as a function of the new variables (PC1 and PC2) is shown, expressed in minutes. Negative values in PC2 values indicate that a number of RPSI grid cells are incompatible with others. A classification of the RPSI grid cells is obtained from PCA: local versus regional (identified by PC1); and regional ones depending on the weather pattern (identified by PC2).

3.3 Temporal range of the regional surface influence

The mean annual residence time of air masses in the surface layer (0–300 m) are 14%, 11%, 4.3% and 1.1% of the total simulation time (96 h) for the release points centered at 600, 1200, 2500 and 4000 m a.s.l., respectively. The RPSI temporal influence is confined during the first 57 h of simulation (600 m a.s.l.) and 21 h (1200 m a.s.l.), that is, double and single diurnal cycles respectively before arriving at the measurement site. At 2500 and 4000 m a.s.l., regional influence is scarcely recovered. These results highlight that simulation times up to 50 h are enough for studies assessing the upwind surface regional influence. This result is in accordance with that reported in Gloor et al. (2001) who found that the timescale over which the imprint of surface fluxes on air masses before arriving at the Wisconsin tower was the order of 1.5 days. This finding also suggests that the choice of 4 days for the backward simulations is adequate to capture the regional surface influence of CO_2 measurements in vertical profiles in NE Spain.

4 Overlap of footprints and application to data

The analysis of the main RPSI for the three aircraft sites belonging to the CAS shows that all vertices have similar footprints (see Sect. 3.2 and Fig. 3) although some differences are visible. Such redundant surface information is important as it allows a better constraint of surface fluxes (Folini et al., 2009) as each measurement is a weighted combination of similar local and regional surface fluxes.

Table 1. Annual and seasonal average (±1 standard deviation) of the Sorensen's Quotient of Similarity (Q/S) for the PSI and the RPSI areas for the three sites belonging to the Linyola's CAS for the set of 51 simulations for 2006.

	PSI	RPSI
600 m a.s.l.		
Annual	94.9±1.2	70.6±2.3
DJF	92.0±3.1	67.5±1.9
MMA	92.9±1.8	66.1±3.3
JJA	96.5±0.6	72.8±4.5
SON	96.8±0.5	75.2±5.3
1200 m a.s.l.		
Annual	95.3±1.4	67.9±1.5
DJF	92.4±3.8	63.3±6.0
MMA	94.0±2.1	59.9±5.5
JJA	96.6±0.3	71.6±3.4
SON	96.9±0.4	74.0±5.0
2500 m a.s.l.		
Annual	93.5±1.2	35.7±12.0
DJF	88.8±2.1	25.4±9.3
MMA	90.3±2.3	19.8±25.3
JJA	95.8±0.6	42.4±9.7
SON	95.8±0.8	50.0±7.6
4000 m a.s.l.		
Annual	90.6±1.3	11.9±14.5
DJF	85.6±3.3	10.0±9.4
MMA	87.1±2.0	–
JJA	93.7±0.3	14.2±22.3
SON	93.0±1.3	10.2±9.6

In order to assess the degree of similarity of the surface influence between sites, the pair-by-pair Sorensen's Quotient of Similarity (Kobayashi, 1987) for the PSI and RPSI is calculated as:

$$Q/S = \frac{2j}{(a+b)} \times 100 \quad (1)$$

where a and b are the PSI (RPSI) area for each of the compared sites, and j is the common PSI (RPSI) area shared by both.

Averaging for the three pair-by-pair comparisons, sites belonging to the same CAS share more than 90% of the PSI area at all altitudes (Table 1). With regards to the RPSI comparison, the shared information decreases to 70% at both 600 m and 1200 m; to 35% at 2500 m and to ∼10% at

4000 m a.s.l. As a whole the 30% unshared RPSI area would introduce the largest variability when comparing measurements carried out in the boundary layer at different sites.

Three aircraft campaigns carried out in 2006 in the Linyola's CAS are shown (Figs. 4–6) in order to analyze the differences in the measured CO_2 concentration between the three vertices in relation to the PSI and RPSI areas of each site. Two of the three flights (February and November) are chosen as they were carried out during cold months and under similar weather conditions (anticyclonic weather). In February the anticyclonic conditions were settled a week before the campaign whereas in November the passage of a cold front occurred the previous day with the wind blowing from S Spain preceding the establishment of a high pressure center in the Iberian Peninsula. Light surface winds (less than 5 m s^{-1}) and mild temperatures (6.6° C and 12.8° C, respectively), were registered for the February and November flight campaigns. The altitude of the PBL determined from radiosounding data at Zaragoza's airport (180 km east of Linyola within the same geographical unit located in the centre of the Ebre watershed) using the Bulk Richardson Number method (Grimsdell and Angevine, 1998; Menut et al., 1999; Eresmaa et al., 2006; Sicard et al., 2006; Morille et al., 2007) was 830 m (February) and 1250 m (November). The third campaign shown in this study took place on 24 August 2006 also under anticyclonic weather but characterized by the passage of a cold front in N Spain and the presence of relatively low pressure centres in the central part of the Iberian Peninsula forcing air masses to spin anticlockwise. Warm temperatures were registered in the Zaragoza airport at 12:00 UTC (∼ 22 °C) with northerly winds of ∼9 m s^{-1}. The PBL height, also determined from the radiosounding data in Zaragoza by the Bulk Richardson Number method, was 1490 m.

The vertical distribution of CO_2 concentrations for the flight in February (Fig. 4a) showed high concentrations at the 600 m level (mean concentration of 397.5 ppmv), and lower concentrations at 1200 m (385.7 ppmv) and 2100 m (383.4 ppmv). The spatial variability of the CO_2 concentration (expressed in terms of one standard deviation) was larger at 600 m (±2.0 ppmv) than at 1200 m and 2200 m (±0.7 ppmv and ±0.2 ppmv respectively).

Similar vertical distribution was observed during the November flight (Fig. 5a): high CO_2 values were recorded at the 600 m level (399.2 ppmv) while values decreased in altitude (385.0 ppmv at 1200 m and 385.6 ppmv at 2100 m). The spatial variability was also larger in the lowest sampled levels (±4.7 ppmv at 600 m and ±1.6 ppmv at 1200 m) whereas the dispersion at 2200 m was lower (±0.6 ppmv).

For the campaign in August, the mean concentration at 600 m was 377.6 ppmv; 378.6 ppmv at 1200 m and 379.7 ppmv at 2200 m. The variability of measurements was similar at the first two levels (±1.3 ppmv) whereas it was ±0.5 ppmv at the highest.

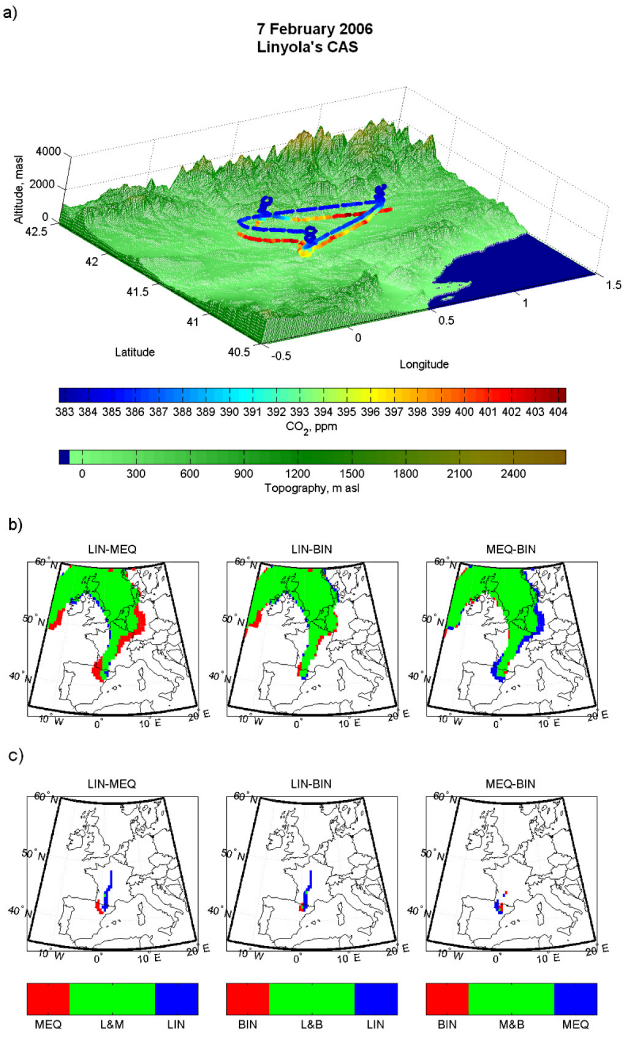

Fig. 4. **(a)** CO_2 mixing ratios measured during the flight on 7 February 2006 superimposed to the topography of the region extracted from GTOPO30 global digital elevation model (DEM) from the US Geological Survey's EROS Data Center in Sioux Falls, South Dakota (http://edc.usgs.gov/). **(b)** Pair-by-pair qualitative differences of the Potential Surface Influence (PSI) between LIN, MEQ and BIN for the simulation started at 7 February 2006 12:00:00 UTC. **(c)** Pair-by-pair qualitative differences of the Regional Potential Surface Influence (RPSI) between LIN, MEQ and BIN for the simulation started at 7 February 2006, 12:00:00 UTC.

The vertical distribution of CO_2 responds to the fact that the signal of the surface fluxes is vertically confined within the PBL. This is also shown by the total residence time in the PSI at different altitudes of the profile. At 600 m a.s.l., the total residence time in the PSI was 18.1 h (February), 12.1 h (August) and 19.8 h (November) whereas at 2200 m a.s.l., it was 0 h (February), 7.9 h (August) and 2.7 h (November). In winter, anthropogenic emissions and respiration fluxes from terrestrial ecosystems caused large CO_2 concentrations near the surface, thus higher concentrations were recorded within

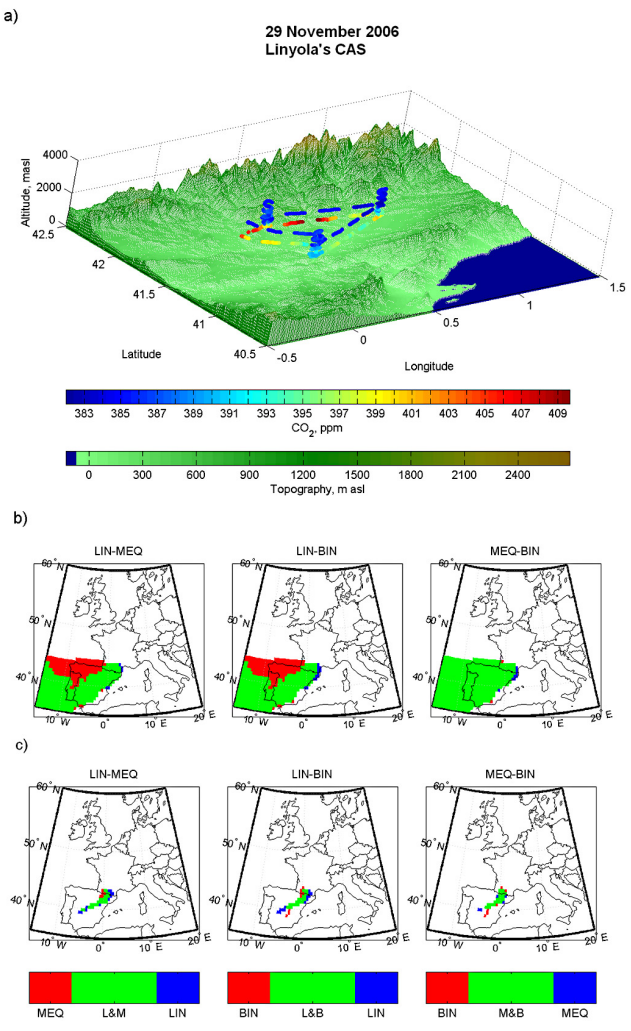

Fig. 5. Same as Fig. 4 but for 29 November 2006.

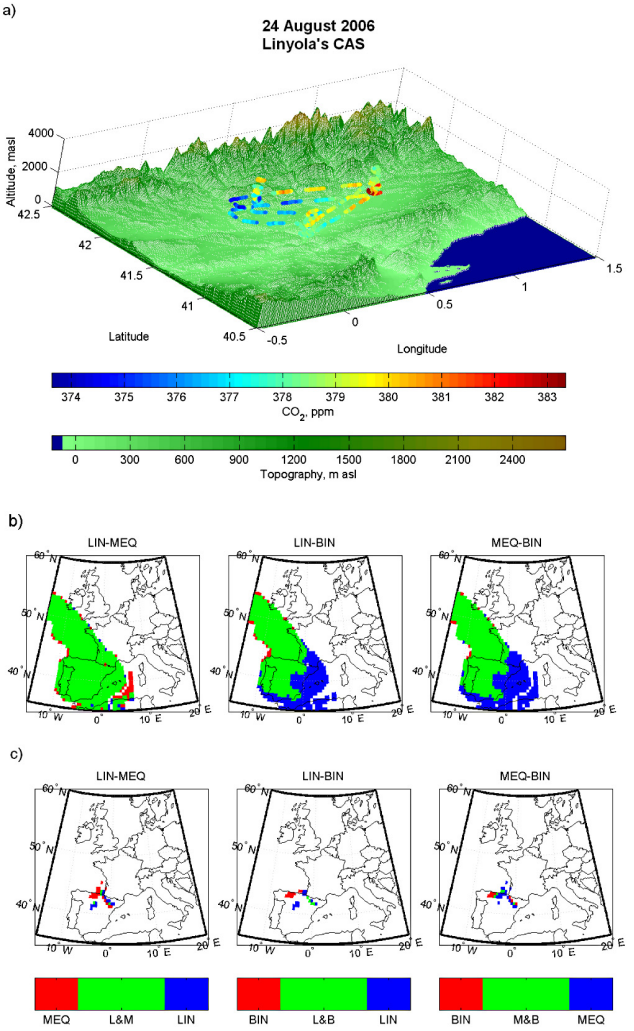

Fig. 6. Same as Fig. 4 but for 24 August 2006.

the PBL compared to those above it. Conversely, larger concentrations were measured above the PBL in summer due to photosynthetic uptake CO_2 from the PBL. The spatial variability was larger in the levels within the PBL as concentrations were more influenced by the variability of local and regional surface fluxes (and also by local turbulent processes, convection and updrafts), than concentrations measured above it. The RPSI was null at 2200 m a.s.l. for the February and November flights, and reduced to 11.6% for the August flight. Conversely, the RPSI at 600 m a.s.l. was 35% (February), 25.8% (August) and 78.0% (November) of the total residence time in the PSI.

The horizontal distribution of the CO_2 mixing ratios at 600 m was different for the three flights. Large CO_2 concentrations (up to 400 ppmv) were detected in the E and NE part of the CAS during the February flight (Fig. 4a) whereas the largest CO_2 concentrations were measured in the N part of the CAS during the November flight, with values up to 410 ppmv (Fig. 5a). For the August flight, the largest CO_2 mixing ratios were measured in the E part of the CAS, with values of 383 ppmv, whereas the CO_2 concentration in the western part of the CAS was 10 ppmv lower (Fig 6a).

In order to explain the CO_2 differences observed in the CAS for three campaigns, the PSI (and RPSI) for the three vertices of the CAS are calculated. The PSI (RPSI) areas for the three vertices of the Linyola's CAS for 7 February 2006, 12:00 UTC at 600 m a.s.l. are displayed in Fig. 4b and c. Even though the three vertices shared 91% of the overall PSI (Fig. 4b), each site had different regional information (RPSI shared area was ∼11%). Air masses contained a northerly component but they crossed the Pyrenees by separate transversal valleys before arriving at each measurement site. Air masses arriving at LIN crossed the Pallaresa valley while those arriving at MEQ crossed the Pyrenees by a more westerly valley, gathering the influence from the upper Ebre watershed. Conversely, BIN showed a very local RPSI influence. The mean RPSI Q/S index value was 11%, the highest being the LIN-BIN comparison (14%) and the lowest, LIN-

MEQ (6%). The CO_2 difference measured at LIN was higher by 0.73 ppmv relative to MEQ; and only 0.05 ppmv lower than BIN. Given that the PSI areas were similar between the three sites and the RPSI regions were located in the Pyrenees (where small CO_2 surface fluxes are expected at that time of the year), the large CO_2 concentrations measured at 600 m a.s.l. are attributed to more local CO_2 fluxes that the meteorological model cannot resolve.

Conversely, for the campaign carried out on the 29 November 2006, sites separated by 60 km shared about 98% (65%) of the PSI (RPSI) area. The PSI area was located in the Iberian Peninsula and the Atlantic Ocean but the RPSI was the central part of the Iberian Peninsula and SW of the Ebre watershed. Despite the large PSI and RPSI similarity index values between vertices, the large surface fluxes caused measured CO_2 differences in the unshared RPSI area belonging to the central part of the Iberian Peninsula containing big cities and industrial areas around the Madrid region. The variability of the surface fluxes at the regional scale (10^4 km^2) influenced the measured CO_2 variability in the lower scale (10^2 km^2).

For the August flight, the PSI area of BIN was the Atlantic Ocean and W-SW of the Iberian Peninsula whereas the southern sites of the CAS (LIN and MEQ) also had influence from the Mediterranean Sea. Looking at the RPSI area, BIN and MEQ were mostly influenced by the central part of the Ebre watershed up to the Cantabria range in the north; and LIN the influence of the Meseta area. The large CO_2 concentrations at LIN compared to MEQ (3.4 ppmv higher) and BIN (5.6 ppmv higher) might be due to the influence from the Meseta region as the western sites of the CAS didn't gather. The smallest CO_2 difference between vertices was between MEQ and BIN (2.2 ppmv), related to the largest RPSI coincidence value (28.7%), rather than that between MEQ and LIN (3.4 ppmv) which exhibited the largest PSI coincidence (92%) but the lowest RPSI Q/S index value (21%).

5 Conclusions

The Potential Surface Influence (PSI) for three sites in NE Spain within the Linyola's Crown Atmospheric Sampling (CAS), separated by 60 km, at four different altitudes (600, 1200, 2500 and 4000 m a.s.l.) for 51 days in 2006, are examined in order analyze the horizontal, vertical and temporal extent of the regional potential surface influence (RPSI) for atmospheric CO_2 mixing ratios to explain measured variability. The application of a residence time threshold criteria in the PSI delimitate the regional surface influence (10^4 km^2) of atmospheric observations and improves the interpretation of the measured differences. The main regional footprint area for these three sites at 600 and 1200 m a.s.l. assures a good spatial coverage of the main land uses in the central part of the Ebre watershed.

Intensive sampling within the boundary layer is needed to cope with spatial CO_2 variability in relation to different land use coverage and vegetation conditions at the regional scale. The measurements carried out on low levels of vertical profiles contain most of the regional CO_2 surface flux signal whilst at high altitudes (2500 m and 4000 m a.s.l.) the regional surface influence is almost reduced to zero. CO_2 mixing ratios above the PBL adhere to a well-mixed latitudinal concentration not influenced by the short-term (hourly to diurnal) regional surface fluxes. Therefore, a single measurement point at 4000 m a.s.l. every 10^2–10^3 km is enough to capture the free troposphere or background CO_2 concentration needed to quantify the enhancements due to regional-scale surface emissions (Folini et al., 2009).

Approximately 40% of the surface influence for measurements done 2200 m a.s.l. is confined in the 10^4 km^2 regional scale up to ∼50 h before the sampling. Measurements within the PBL are influenced by two complete diurnal cycles of terrestrial fluxes in the regional field (photosynthesis/respiration diurnal cycle) and by the boundary layer diurnal evolution.

The differences in the measured CO_2 concentration between vertices of the CAS could be assessed by differences on the RPSI area. Although sites that are separated by 60 km are sensible to similar surface fluxes (PSI Sorensen's Quotient Similarity index reach values up to 90%) differences in the CO_2 concentration appeared attributable to differences in the unshared RPSI regions. Dissimilant, in the measured CO_2 concentration between the vertices of the CAS are due to very local surface fluxes (as in the February flight) or due to the variability of the RPSI area with large surface fluxes (as in the November and August flights).

The dominance of the surrounding field contributions over daytime mixing ratios of CO_2 has an impact on inversion studies as a small bias in the assumed flux in the near field can bring a large bias in the modelled mixing ratio when only one measurement site is considered (Gerbig et al., 2009). A compensatory effect arises when using multiple sites in a network: a local bias in fluxes at one measurement location represents a small bias for another measurement site some distance away. A dense network of tower and aircraft observations with overlapping footprints in both surface area and vegetation class are needed to provide reliable regional CO_2 budgets. Overlapping coincidences within a network of measurement sites (as presented in this study) represent independent observations containing the same CO_2 regional surface flux information. The vertices of the CAS at 600 and 1200 m a.s.l. show an average overlapping value of 90% for the PSI and 70% for the RPSI. This configuration will increase the ability to assess the CO_2 regional carbon budget in NE Spain. The CAS design also brings information of the representation error in inversion models as it handles with the variability of a typical grid cell. The representation error could reach values of ∼5 ppmv as shown in the November flight at 600 m a.s.l.

Acknowledgements. We would like to thank all the people who made possible the Aircraft Measurement Programs in Spain (ICARO and ICARO-II) and especially M. A. Rodríguez, I. Pouchet and the crew of Top Fly, Sunfly and A. Lapetra. The authors want also to thank the NOAA-ESRL-GMD Research Group and especially A. Hirsch, G. Pétron and C. Sweeny for the discussion on the FLEXPART model. Thanks are due to M. Priestman for the English corrections and to two anonymous reviewers for their suggestions and comments. This research was funded by the Spanish Ministry of Education and Science (projects REN2003-06089 and GL12398).

Edited by: A. Stohl

References

Aalto, T., Hatakka, J., Paatero, J., Tuovinen, J.-P., Aurela, M., Laurila, T., Holmén, K., Trivett, N., and Viisanen, Y.: Tropospheric carbon dioxide concentrations at a northern boreal site in Finland: basic variations and source areas, Tellus, 54B, 110–126, 2002.

Ahmadov, R., Gerbig, C., Kretschmer, R., Körner, S., Rödenbeck, C., Bousquet, P., and Ramonet, M.: Comparing high resolution WRF-VPRM simulations and two global CO_2 transport models with coastal tower measurements of CO_2, Biogeosciences, 6, 807–817, doi:10.5194/bg-6-807-2009, 2009.

Apadula, F., Gotti, A., Pigini, A., Longhetto, A., Rocchetti, F., Cassardo, C., Ferrarese, F., and Forza, R.: Localization of source and sink regions of carbon dioxide through the method of the synoptic air trajectory statistics, Atmos. Environ., 37, 3757–3770, 2003.

Ashbaugh, L. L., Myrup, L. O., and Flocchinim, R. G.: A principal component analysis of sulfur concentrations in the western United States, Atmos. Environ., 18, 783–791, 1984.

Aubinet, M., Chermanne, B., Vandenhaute, M., Longdoz, B., Yernaux, M., and Laitat, E.: Long term carbon dioxide exchange above a mixed forest in the Belgian Ardennes, Agr. Forest Meteorol., 108, 293–315, 2001.

Bakwin, P. S., Tans, P. P., Stephens, B. B., Wofsy, S. C., Gerbig, C., and Grainger, A.: Strategies for measurement of atmospheric column means of carbon dioxide from aircraft using discrete sampling, J. Geophys. Res., 108(D16), 4514, doi:10.1029/2002JD003306, 2003.

Baldocchi, D., Falge, E., Gu, L., Olson, R., Hollinger, D., Running, S., Anthoni, P., Bernhofer, Ch., Davis, K., Evans, R., Fuentes, J., Goldstein, A., Katul, G., Law, B., Lee, X., Malhi, Y., Meyers, T., Munger, W., Oechel, W., Paw, U. K. T., Pilegaard, K., Schmid, H. P., Valentini, R., Verma, S., Vesala, T., Wilson, K., and Wofsy, S.: FLUXNET: A new tool to study the temporal and spatial variability of ecosystem – scale carbon dioxide, water vapor and energy flux densities, B. Am. Meteorol. Soc., 82(11), 2415–2434, 2001.

Blanchard, C.: Methods for attributing ambient air pollutants to emission source, Annual Rev. Energy Environ., 24, 329–365, 1999.

Bousquet, P., Ciais, P., Peylin, P., Ramonet, M., and Monfray, M.: Inverse modeling of annual atmospheric CO_2 sources and sinks, 1. Method and control inversion, J. Geophys. Res., 104(D21), 26161–26178, 1999.

Canadell, J. G, Mooney, H. A., Baldocchi, D. D., Berry, J. A., Ehleringer, J. R., Field, C. B., Gower, S. T., Hollinger, D. Y., Hunt, J. E., Jackson, R. B., Running, S. W., Shaver, G. R., Steffen, W., Trumbore, S. E., Valentini, R., and Bond, B. Y.: Carbon metabolism of the terrestrial biosphere: a multitechnique approach for improved understanding, Ecosystems, 3, 115–130, 2000.

Choi, Y., Vay, S. A., Vadrevu, K. P., Soja, A. J., Woo, J.-H., Nolf, S. R., Sachse, G. W., Diskin, G. S., Blake, D. R., Blake, N. J., Singh, H. B., Avery, M. A., Fried, A., Pfister, L., and Fuelberg, H. E.: Characteristics of the atmospheric CO_2 signal as observed over the conterminous United States during INTEX-NA, J. Geophys. Res., 113, D07301, doi:10.1029/2007JD008899, 2008.

Ciais, P., Tans, P. P., Trolier, M., White, J. W. C., and Francey, R. J.: A Large Northern Hemisphere Terrestrial CO_2 Sink Indicated by the $^{13}C/^{12}C$ Ratio of Atmospheric CO_2, Science, 269, 1098–1102, doi:10.1126/science.269.5227.1098, 1995.

Corbin, K. D., Denning, A. S., Lu, L., Wang, J.-W., and Baker, I. T.: Possible representation errors in inversions of satellite CO_2 retrievals, J. Geophys. Res.-Atmos., 113, D02301, doi:10.1029/2007JD008716, 2008.

Denning, A. S., Zhang, N., Yi, C., Branson, M., Davis, K., Kleist, J., and Bakwin, P.: Evaluation of modeled atmospheric boundary layer depth at the WLEF tower, Agr. Forest Meteorol., 148, 206–215, 2008.

Dolman, A. J., Noilhan, J., Durand, P., Sarrat, C., Brut, A., Piguet, B., Butet, A., Jarosz, N., Brunet, Y., Loustau, D., Lamaud, E., Tolk, L., Ronda, R., Miglietta, F., Gioli, B., Magliulo, V., Esposito, M., Gerbig, C., Körner, S., Glademard, P., Ramonet, M., Ciais, P., Neininger, B., Hutjes, R. W. A., Elbers, J. A., Macatangay, R., Schrems, O., Pérez-Landa, G., Sanz, M. J., Scholz, Y., Facon, G., Ceschia, E., and Beziat, P.: The CarboEurope Regional Experiment Strategy, B. Am. Meteorol. Soc., 10, 1367–1379, doi:10.1175/BAMS-87-10-1367, 2006.

Dolman, A. J., Gerbig, C., Noilhan, J., Sarrat, C., and Miglietta, F.: Detecting regional variability in sources and sinks of carbon dioxide: a synthesis, Biogeosciences, 6, 1015–1026, doi:10.5194/bg-6-1015-2009, 2009.

Eresmaa, N., Karppinen, A., Joffre, S. M., Räsänen, J., and Talvitie, H.: Mixing height determination by ceilometer, Atmos. Chem. Phys., 6, 1485–1493, doi:10.5194/acp-6-1485-2006, 2006.

Fan, S., Gloor, M., Mahlman, J., Pacala, S., Sarmiento, J., Takahashi, T., and Tans, P.: A Large Terrestrial Carbon Sink in North America Implied by Atmospheric and Oceanic Carbon Dioxide Data and Models, Science, 282, 442–446, doi:10.1126/science.282.5388.442, 1998.

Folini, D., Kaufmann, P., Ubl, S., and Henne, S.: Region of influence of 13 remote European measurement sites based in modeled carbon monoxide mixing ratios, J. Geophys. Res., 114, D08307, doi:10.1029/2008JD011125, 2009.

Font, A., Morgui, M. J., and Rodo, X.: Atmospheric CO_2 in-situ measurements: two examples of Crown Design flights in NE Spain, J. Geophys. Res., 113, D12308, doi:10.1029/2007JD009111, 2008.

Font, A., Morgui, J.-A., Curcoll, R., Pouchet, I., Casals, I., and Rodo, X.: Daily carbon surface fluxes in the West Ebre (Ebro) watershed from aircraft profiling on late June 2007, Tellus B, 62,

427–440, doi:10.1111/j.1600-0889.2010.00469.x, 2010.

Gerbig, C., Lin, J. C., Wofsy, S. C., Daube, B. C., Andrews, A. E., Stephens, B. B., Bakwin, P. S., and Grainger C. A.: Toward constraining regional-scale fluxes of CO_2 with atmospheric observations over a continent: 1. Observed spatial variability from airborne platforms, J. Geophys. Res., 108(D24), 4756, doi:10.1029/2002JD003018, 2003a.

Gerbig, C., Lin, J. C., Wofsy, S. C., Daube, B. C., Andrews, A. E., Stephens, B. B., Bakwin, P. S., and Grainger, C. A.: Toward constraining regional-scale fluxes of CO_2 with atmospheric observations over a continent: 2. Analysis of COBRA data using a receptor-oriented framework, J. Geophys. Res., 108(D24), 4757, doi:10.1029/2003JD003770, 2003b.

Gerbig, C., Körner, S., and Lin, J. C.: Vertical mixing in atmospheric tracer transport models: error characterization and propagation, Atmos. Chem. Phys., 8, 591–602, doi:10.5194/acp-8-591-2008, 2008.

Gerbig, C., Dolman, A. J., and Heimann, M.: On observational and modelling strategies targeted at regional carbon exchange over continents, Biogeosciences, 6, 1949–1959, doi:10.5194/bg-6-1949-2009, 2009.

Gloor, M., Bakwin, P., Hurst, D., Lock, L., Draxler, R., and Tans, P.: What is the concentration footprint of a tall tower?, J. Geophys. Res., 106(D16), 17831–17840, 2001.

Grimsdell, A. and Angevine, W. M.: Convective Boundary Layer Height Measurement with Wind Profilers and Comparison to Cloud Base, J. Atmos. Oceanic Technol., 15, 1331–1338, 1998.

Gurney, K. R., Law, R. M., Denning, A. S., Rayner, P. J., Baker, D., Bousquet, P., Bruhwiller, L., Chen, Y.-H., Ciais, P., Fan, S., Fung, I. Y., Gloor, M., Heimann, M., Higuchi, K., John, J., Maki, T., Maksyutov, S., Masarie, K., Peylin, P., Prather, M., Pak, B. C., Randerson, J., Sarmiento, J., Taguchi, S., Takahashi, T., and Yuen, C.-W.: Towards robust regional estimates of CO_2 sources and sinks using atmospheric transport models, Nature, 415, 626–630, 2002.

Gurney, K. R., Baker, D., Rayner, P., and Denning, S.: Interannual variations in continental-scale net carbon exchange and sensitivity to observing networks estimated from atmospheric CO_2 inversions for the period 1980 to 2005, Global Biogeochem. Cy., 22, GB3025, doi:10.1029/2007GB003082, 2008.

Henne, S., Brunner, D., Folini, D., Solberg, S., Klausen, J., and Buchmann, B.: Assessment of parameters describing representativeness of air quality in-situ measurement sites, Atmos. Chem. Phys., 10, 3561–3581, doi:10.5194/acp-10-3561-2010, 2010.

Jorba, O., Pérez, C., Rocadenbosch, F., and Baldasano, J.: Cluster Analysis of 4-Day Back Trajectories Arriving in the Barcelona Area, Spain, from 1997 to 2002, Amer. Meteorol. Soc., 43, 887–901, 2004.

Kobayashi, S.: Heterogenity Ratio: a measure of beta-diversity and its use in community classification, Ecol. Res., 2, 101–111, 1987.

Lafont, S., Kergoat, L., Dedieu, G., Chevillard, A., Karstens, U., and Kolle, O.: Spatial and temporal variability of land CO_2 fluxes estimated with remote sensing and analysis data over western Eurasia, Tellus, 54B, 820–833, 2002.

Lin, J. C. and Gerbig, C.: Accounting for the effect of transport errors on tracer inversions, Geophys. Res. Lett., 32, L01802, doi:10.1029/2004GL021127, 2005.

Lin, J. C., Gerbig, C., Wofsy, S. C., Andrews, A. E., Daube, B. C., Grainger, C. A. Stephens, B. B., Bakwin, P. S., and Hollinger, D. Y.: Measuring fluxes of trace gases at regional scales by Lagrangian observations: Application to the CO_2 Budget and Rectification Airborne (COBRA) study, J. Geophys. Res., 109, D15304, doi:10.1029/2004JD004754, 2004.

Liu, S. C. and McAfee, J. R: Radon 222 and tropospheric vertical transport, J. Geophys. Res., 89(D5), 7291–7297, 1984.

Lloyd, J., Francey, R. J., Mollicone, D., Raupach, M. R., Sogachev, A., Arneth, A., Byers, J. N., Kelliher, F. M., Rebmann, C., Valentini, R., Wong, S.-C., Bauer, G., and Schulze, E.-D.: Vertical profiles, boundary layer budgets, and regional flux estimates for CO_2, and its 13C/12C ratio for water vapour above a forest/bog mosaic in central Siberia, Glob. Biogeochem. Cyc., 15, 267–284, 2001.

Lloyd, J., Langenfelds, R., Francey, R. J., Gloor, M., Tschebakova, N. N., Zolotukhine, D., Werner, R. A., Jordan, A., Allison, C. A., Zrazhewske, V., Shibistova, O., and Schulze, E. D.: A trace gas climatology above Zotino, central Siberia, Tellus, 54B, 590–610, 2002.

Lloyd, J., Kolle, O., Fritsch, H., de Freitas, S. R., Silva Dias, M. A. F., Artaxo, P., Nobre, A. D., de Araújo, A. C., Kruijt, B., Sogacheva, L., Fisch, G., Thielmann, A., Kuhn, U., and Andreae, M. O.: An airborne regional carbon balance for Central Amazonia, Biogeosciences, 4, 759–768, doi:10.5194/bg-4-759-2007, 2007.

Marquis, M. and Tans, P.: Carbon Crucible, Science, 320, 460–461, 2008.

Martins, D. K., Sweeny, C., Stirm, B. H., and Shepson, P. B.: Regional surface flux of CO_2 inferred from changes in the advected CO_2 column density, Agric. Forest Meteorol., 149(10), 1674–1685, 2009.

Menut, L., Flamant, C., Pelon, J., and Flamant, P. H.: Urban boundary-layer height determination from lidar measurements over the Paris area, Appl. Opt. Lp., 38, 945–954, 1999.

Morille, Y., Haeffelin, M., Drobinski, P., and Pelon, J.: STRAT: An automated algorithm to retrieve the vertical structure of the atmosphere from single-channel lidar data, J. Atmos. Oceanic Technol., 24, 761–775, 2007.

Overland J. E. and Preisendorfer, R. W.: A significance test for principal components applied to a cyclone climatology, Mon. Wea. Rev., 110, 1–4, 1982.

Papale, D. and Valentini, A.: A new assessment of European forests carbon exchanges by eddy fluxes and artificial neural network spatialization, Glob. Change Biol., 9, 525–535, 2003.

Paris, J.-D., Stohl, A., Ciais, P., Nédélec, P., Belan, B. D., Arshinov, M. Yu., and Ramonet, M.: Source-receptor relationships for airborne measurements of CO_2, CO and O_3 above Siberia: a cluster-based approach, Atmos. Chem. Phys., 10, 1671–1687, doi:10.5194/acp-10-1671-2010, 2010.

Peters, W., Jacobson, A. R., Sweeney, C., Andrews, A. E., Conway, T. J., Masarie, K., Miller, J. B., Bruhwiler, L. M. P., Pétron, G., Hirsch, A. I., Worthy, D. E. J., van der Werf, G. R., Randerson, J. T., Wennberg, P. O., Krol, M. C., and Tans, P. P.: An atmospheric perspective on North American carbon dioxide exchange: CarbonTracker, Proc. Natl. Acad. Sci., 104, 48, 18925–18930, 2007.

Peters, W., Krol, M. C., Van Der Werf, G. R., Houweling, S., Jones, C. D., Hughes, J., Schaefer, K., Masarie, K. A., Jacobson, A. R., Miller, J. B., Cho, C. H., Ramonet, M., Schmidt, M., Ciattaglia, L., Apadula, F., Heltai, D., Meinhardt, F., Di Sarra, A. G., Piacentino, S., Sferlazzo, D., Aalto, T., Hatakka, J., Ström, J.,

Haszpra, L., Meijer, H. A. J., Van Der Laan, S., Neubert, R. E. M., Jordan, A., Rodó, X., Morguí, J. A., Vermeulen, A. T., Popa, E., Rozanski, K., Zimnoch, M., Manning, A. C., Leuenberger, M., Uglietti, C., Dolman, A. J., Ciais, P., Heimann, M., and Tans, P. P.: Seven years of recent net terrestrial carbon dioxide exchange over Europe constrained by atmospheric observations, Glob. Change Biol.,16, 1317–1337, doi:10.1111/j.1365-2486.2009.02078.x, 2009.

Rannik, Ü., Aubinet, M., Kurbanmuradov, O., Sabelfeld, K. K., Markkanen, T., and Vesala, T.: Footprint analysis for measurements over a heterogeneous forest, Bound.-Lay. Meteorol., 97, 137–166, 2000.

Running, S. W., Nemani, R. R., Heinsch, F. A., Zhao, M. S., Reeves, M., and Hashimoto, H.: A continuous satellite-derived measure of global terrestrial primary production, Bioscience, 54, 547–560, 2004.

Sarrat, C., Noilhan J., Lacarrère, P., Donier, S., Lac, C., Calvet, J. C., Dolman, A. J., Gerbig, C., Neininger, B., Ciais, P., Paris, J. D., Boumard, F., Ramonet, M., and Butet, A.: Atmospheric CO_2 modeling at the regional scale: Application to the CarboEurope Regional Experiment, J. Geophys. Res., 112, D12105, doi:10.1029/2006JD008107, 2007a.

Sarrat, C., Noilhan, J., Dolman, A. J., Gerbig, C., Ahmadov, R., Tolk, L. F., Meesters, A. G. C. A., Hutjes, R. W. A., Ter Maat, H. W., Pérez-Landa, G., and Donier, S.: Atmospheric CO_2 modeling at the regional scale: an intercomparison of 5 meso-scale atmospheric models, Biogeosciences, 4, 1115–1126, doi:10.5194/bg-4-1115-2007, 2007b.

Sarrat, C., Noilhan, J., Lacarrère, P., Masson, V., Ceschia, E., Ciais, P., Dolman, A., Elbers, J., Gerbig, C., and Jarosz, N.: CO_2 budgeting at the regional scale using a Lagrangian experimental strategy and meso-scale modeling, Biogeosciences, 6, 113–127, doi:10.5194/bg-6-113-2009, 2009.

Schmitgen, S., Geiß, H., Ciais, P., Neininger, B., Brunet, Y., Reichstein, M., Kley, D., and Volz-Thomas, A.: Carbon dioxide uptake of a forested region in southwest France derived from airborne CO_2 and CO measurements in a quasi-Lagrangian experiment, J. Geophys. Res., 109, D14302, doi:10.1029/2003JD004335, 2004.

Seibert, P. and Frank, A.: Source-receptor matrix calculation with a Lagrangian particle dispersion model in backward mode, Atmos. Chem. Phys., 4, 51–63, doi:10.5194/acp-4-51-2004, 2004.

Shashkov, A., Higuchi, K., and Chan, D.: Aircraft profiling of variation of CO_2 over a Canadian Boreal Forest Site: a role of advection in the changes in the atmospheric boundary layer CO_2 content, Tellus, 59B, 234–243, doi:10.1111/j.1600-0889.2006.00237.x, 2007.

Sicard, M., Pérez, C., Rocadenbosch, F., Baldasano, J. M., and García-Vizcaino, D.: Mixed-layer depth determination in the Barcelona Coastal area from regular Lidar measurements: methods, results and limitations, Bound.-Layer Meteor., 119, 135–157, 2006.

Sidorov, K., Sogachev, A., Langendörfer, U., Lloyd, J., Nepomnjashiy, I. L., Vygodskaya, N., Schmidt, M., and Levin, I.: Seasonal variability of greenhouse gases in the lower troposphere above the eastern European Taïga (Syktyvkar, Russia), Tellus, 54B, 735–748, 2002.

Stohl, A. and Thomson, D. J.: A density correction for Lagrangian Particle Dispersion models, Bound-Lay. Meteorol., 90, 155–167, 1999.

Stohl, A., Eckhardt, S., Forster, C., James, P., and Spichtinger, N.: On the pathways and timescales of intercontinental air pollution transport, J. Geophys. Res., 107(D23), 4684, doi:10.1029/2001JD001396, 2002.

Stohl, A., Forster, C., Eckhardt, S., Spichtinger, N., Huntrieser, H., Heland, J., Schlager, H., Wilhelm, S., Arnold, F., and Cooper, O.: A backward modeling study of intercontinental transport using aircraft measurements, J. Geophys. Res., 108(D12), 4370, doi:10.1029/2002JD002862, 2003.

Stohl, A., Forster, C., Frank, A., Seibert, P., and Wotawa, G.: Technical note: The Lagrangian particle dispersion model FLEXPART version 6.2, Atmos. Chem. Phys., 5, 2461–2474, doi:10.5194/acp-5-2461-2005, 2005.

Sun, J., Oncley, S. P., Burns, S. P., Stephens, B. B., Lenschow, D. H., Campos, T., Monson, R. K., Schimel, D. S., Sacks, W. J., De Wekker, S. F. J., Lai, C.-T., Lamb, B., Ojima, D., Ellsworth, P. Z., Sternberg, L. S. L., Zhong, S., Clements, C., Moore, D. J. P., Anderson, D. E., Watt, A. S., Hu, J., Tschudi, M., Aulenbach, S., Allwine, E., and Coons, T.: A Multiscale and Multidisciplinary Investigation Of Ecosystem – Atmosphere CO_2 Exchange Over the Rocky Mountains of Colorado, Bull. Amer. Meteor. Soc., 91, 209–230, 2010.

Taubman, B. F., Hains, J. C., Thompson, A. M., Marufu, L. T., Doddridge, B. G., Stehr, J. W., Piety, C. A., and Dickerson R. R.: Aircraft vertical profiles of trace gas and aerosol pollution over the mid-Atlantic United States: Statistics and meteorological cluster analysis, J. Geophys. Res., 111, D10S07, doi:10.1029/2005JD006196, 2006.

Tolk, L. F., Meesters, A. G. C. A., Dolman, A. J., and Peters, W.: Modelling representation errors of atmospheric CO_2 mixing ratios at a regional scale, Atmos. Chem. Phys., 8, 6587–6596, doi:10.5194/acp-8-6587-2008, 2008.

van der Molen, M. K. and Dolman, A. J.: Regional carbon fluxes and the effect of topography on the variability of atmospheric CO_2, J. Geophys. Res.-Atmos., 112, D01104, doi:10.1029/2006JD007649, 2007.

Wofsy, S. C., Harriss, R. C., and. Kaplan, W. A.: Carbon dioxide in the atmosphere over the Amazon basin, J. Geophys. Res., 93(D2), 1377–1387, 1988.